Core Physics Analysis in Support of the FNR HEU-LEU Demonstration Experiment

David C. Losey, Forrest B. Brown, William R. Martin
and John C. Lee
Department of Nuclear Engineering
The University of Michigan

Abstract

A core neutronics analysis has been undertaken to assess the impact of low-enrichment fuel on the performance and utilization of the FNR. As part of this analytic effort a computer code system has been assembled which will be of general use in analyzing research reactors with MTR-type fuel. The code system has been extensively tested and verified in calculations for the present high enrichment core. The analysis presented here compares the high-and-low enrichment fuels in batch and equilibrium core configurations which model the actual FNR operating conditions. The two fuels are compared for cycle length, fuel burnup, and flux and power distributions, as well as for the reactivity effects which are important in assessing the impact of LEU fuel on reactor shutdown margin.

Presented at the International Meeting, Reduced-Enrichment Fuels Research and Test Reactors, Argonne National Laboratory, November 12-14, 1980.

1. INTRODUCTION

The University of Michigan Department of Nuclear Engineering and the Michigan-Memorial Phoenix Project are engaged in a cooperative effort with Argonne National Laboratory to test and analyze low enrichment fuel in the Ford Nuclear Reactor. The effort is one element of the Reduced Enrichment Research and Test Reactor (RERTR) Program, which is itself one facet of the overall U.S. policy seeking to minimize the risk of nuclear weapons proliferation. A near-term objective of the RERTR program is to demonstrate and implement enrichment reductions from 93% to less than 20% or, where that is impractical, to 45% within the next two years, based on currently qualified fuel fabrication technology. A part of the effort to meet this objective is a whole-core demonstration with reduced enrichment fuel, which will allow detailed testing and evaluation of the low enrichment fuel and an assessment of its impact on research and test reactor performance and utilization.

The Ford Nuclear Reactor (FNR) at The University of Michigan has been selected for the low-power whole-core demonstration. This demonstration project includes development of methods to analyze MTR-type fuel and core configurations, assisting in the design and analysis of the low enrichment uranium (LEU) fuel, preparation of fuel procurement specifications, preparing the requisite safety analysis report revision and license amendment application, procuring the operating license amendment, planning and conducting the experimental program, and analyzing the results of the experiments, including comparisons with analytical predictions.

The demonstration project at The University of Michigan has been divided into several phases. The initial phase, which is essentially complete, includes the work necessary to design and specify the fuel and obtain the necessary license amendments. The LEU fuel has been designed and is presently being frabricated by two European vendors, NUKEM and CERCA. The LEU fuel elements have a 167.3 gram fissile loading, which is 19.5% higher than the present high enrichment uranium (HEU) fuel. The initial phase of the demonstration project has also included an experimental program to characterize the current HEU core to provide a basis for comparison with the LEU core. In addition, experimental techniques and equipment are being tested and refined during this phase. A companion paper[1] presented at this conference provides further discussion of the experimental portions of this project. The major task of the project will be the actual whole-core testing of the LEU fuel along with the necessary measurements and analysis of experimental results and comparison with analytical predictions performed prior to core loading. The present project schedule calls for actual loading of LEU fuel elements in April, 1981. Further verification and improvement of our calculational methods will also be performed along with the whole-core testing program. Thus at the conclusion of the demonstration project, the impact of LEU fuel on the FNR performance and utilization will be assessed experimentally and compared with analytic predictions using methods developed and implemented during this investigation.

This paper presents a detailed review of the analytical effort performed at The University of Michigan as a part of the demonstration project. While many of our analytic results and methods have been summarized

in earlier conference and project reports[2-6], a detailed summary of the effort to date should be of use to the research reactor community. It is hoped that this review will provide guidance to others planning similar enrichment reductions and an appreciation of the practical considerations in performing detailed reactor analyses which cannot be addressed in generic studies. The following sections present a description of the calculational methods used in the physics analysis, and comparisons of the analysis and measurements used to validate the calculational model for the present high enrichment uranium fuel. We also present comparisons of the physics analyses for the HEU and LEU fuels, a summary of current efforts, and our conclusions to date.

The FNR currently uses highly enriched uranium MTR-type fuel. To provide the means for a valid prediction of the impact of LEU fuel on FNR operation, safety, and research usage, a generic neutronics model has been developed. This model is based on standard, well-verified production codes which are routinely used in reactor analyses. These codes have been modified only when necessary to accommodate the special characteristics of small low-power research reactors with plate-type fuel. As such, the methods of analysis should be applicable to a large number of research reactors and accessible to many computing installations. The following sections provide a brief description of the calculational model and its verification.

II. CALCULATIONAL METHODS

A. Computer Codes

All analyses were performed with the standard, well-verified production codes LEOPARD[7], EPRI-HAMMER[8], 2DB[9], ANISN[10], TWOTRAN[11], and VENTURE.[12]

Brief descriptions of code capabilities are:

1) LEOPARD - a zero-dimensional unit-cell code using the MUFT/SOFOCATE scheme (54 fast and 172 thermal groups); has depletion capability; cross-section library consists of an early industrial data set.
2) EPRI-HAMMER - a one-dimensional integral transport theory code using 54 fast and 30 thermal groups; cross-section library constructed from ENDF/B-IV data.
3) 2DB - a two-dimensional multi-group diffusion theory code with depletion capability.
4) ANISN - a one-dimensional discrete ordinates transport theory code.
5) TWOTRAN-II - a two-dimensional discrete ordinates transport theory code.
6) VENTURE - a three-dimensional multi-group diffusion theory code.

B. Code Modifications

The LEOPARD code originally performed a spectrum calculation for lattices consisting of cylindrical fuel rods. The code was modified to allow slab geometry and separate few-group edits for both lattice and non-lattice regions. The principal modification was in the calculation of thermal disadvantage factors by the ABH method for slab geometry.[13] A summary of these modifications is given in Table 1.

Table 1 Modifications to the LEOPARD Code

Modification	Purpose	Method
slab geometry option	analysis of plate-type fuel	- ABH method for thermal disadvantage factors for slabs - volume fractions, mean chord length, Dancoff factor redefined for slabs - minor input changes
lattice/non-lattice edits	allow separate few-group constants for lattice and inactive side plates	neutron conservation, with separate disadvantage factors for lattice region
xenon cross section edits	allows space-dependent xenon calculation in 2DB	transmit σ_a^{Xe} and Σ_a^{Xe} to 2DB
output few-group constant tablesets as functions of depletion	-automate data transfer to 2DB -allow interpolation in 2DB based on depletion	create output file compatible with modified 2DB
restart capability	allow parametric calculations at any depletion step	save all parameters needed to re-initialize code
added thermal expansion coefficient for Al	allow thermal expansion of meat and clad	minor addition to input routine
allow input multiplier for fission product buildup factor	burnup >> commercial reactor, correlation in code must be extended	minor input change
option for burnup dependent NLPF input	incorporate spectral effects of flux peaking variations due to burnup	minor input changes

The modified LEOPARD code compares satisfactorily with the EPRI-HAMMER code, an accurate, well-verified code used in the analysis of benchmark critical experiments. A typical comparison of k_∞ and two-group parameters in Table 2 shows that despite the many engineering approximations in the LEOPARD code, it compares quite well with the more accurate HAMMER code. Differences in few-group constants are due primarily to differences in the cross-section libraries - HAMMER uses ENDF/B-IV data while LEOPARD uses an early industrial data set.

The 2DB code has been modified to allow a macroscopic depletion capability via interpolation of macroscopic cross sections as a function of depletion. In addition, the isotopic balance equations for xenon and iodine have been included to allow the correct xenon levels within the core as a function of position and time (and macroscopic absorption cross sections are appropriately modified). Other modifications to 2DB have been aimed at automating data handling, improving fuel shuffling and edit capabilities, and greatly decreasing the computer run-time costs. These modifications are summarized in Table 3.

C. Basic Calculation Method

The LEOPARD and 2DB codes were used for routine calculations of core reactivity, depletion effects, and power and flux distributions. Special methods for control rods and core leakage flux are described in subsequent sections. For both HEU and the proposed LEU fuel, the following scheme was used:

Table 2 Comparison of LEOPARD and HAMMER Results for MTR-type Fuel

	93% Alloy		19.5% UAl_x	
	LEOPARD	HAMMER	LEOPARD	HAMMER
k_∞	1.5477	1.5500	1.5150	1.5116
ϕ_1/ϕ_2	2.41	2.40	2.76	2.75
Age	51.5	49.9	49.1	47.5
D_1	1.434	1.372	1.424	1.360
Σ_{a1}	0.00204	0.00182	0.00358	0.00344
Σ_{r1}	0.0258	0.0257	0.0254	0.0253
$\nu\Sigma_{f1}$	0.00206	0.00223	0.00256	0.00274
D_2	0.284	0.272	0.280	0.269
Σ_{a2}	0.0597	0.0594	0.0676	0.0668
$\nu\Sigma_{f2}$	0.0948	0.0935	0.110	0.108

Table 3 Modifications to 2DB

Modification	Purpose	Method
determine macroscopic cross-sections by interpolation based on local fuel burnup	model fuel number density changes and spectrum effects due to local fuel depletion	quadratic Lagrangian interpolation in cross-section tableset from LEOPARD at each depletion step major input options added, extra scratch file and memory
space-dependent xenon	xenon feedback	N^{Xe} determined from local power and flux levels σ_a^{Xe} interpolated as function of local fuel depletion Σ_a^{Xe} added to Xe-free Σ_a
dynamic memory allocation	reduced core storage requirements	system routines acquire only needed space
interface with LEOPARD	reduced input setup	A special preprocessor (LINX) converts LEOPARD cross section sets to the 2DB input format
FIDO input processor	free-format input with many options	total revision of input routines
recoding of inner iteration routines	reduce CPU time by factor of 4	use of precomputed constant arrays to eliminate redundant calculations
improved edits and output	detailed analysis of reaction rates, neutron balance	neutron conservation equations
complete recoding and updating of entire code	improve and clarify coding, reduced storage and CPU time, consolidate all changes	mnemonic variable names, structured programming, improved code logic.

1) The LEOPARD code was used to generate few-group cross sections. For most applications, two energy groups (fast and thermal) were used, although four energy groups were chosen for several detailed calculations.

The geometry chosen was a unit cell in slab geometry consisting of a lattice region and a non-lattice or extra region. The lattice region was composed of fuel meat, clad and water channel. For regular assemblies, the extra region consisted of the side plates, non-active portions of fuel plates, and inter-assembly water gaps, which are homogenized on a volume basis. For special fuel assemblies, the central water hole was also included in the extra region. Few-group macroscopic cross-section sets were generated as functions of depletion for the lattice and non-lattice regions and the total assembly.

For the water reflector and heavy water tank, the extra region was chosen as H_2O or D_2O with a .25% H_2O content and a volume fraction arbitrarily set equal to that of the lattice region. The extra region few-group cross sections obtained in this manner were used for the reflector and heavy water tank in the subsequent global calculation.

2) Global diffusion theory calculations were performed with the 2DB code. Three spatial mesh descriptions were used in x-y geometry. A homogeneous description, with a 2x2 mesh per assembly, was used for survey calculations, equilibrium core studies, and cycle length studies. A discrete representation, using a 6x6 mesh per

assembly with the lattice and non-lattice portions of an assembly explicitly represented, was used for detailed analysis of power and flux distributions, temperature coefficient, and control rod reactivity worth. A discrete representation with a 12x12 mesh per assembly was used for verifying the adequacy of the 2x2 and 6x6 representations, and for comparison with the measured flux distributions. The various mesh structures are presented in Figure 1.

Depletion was accounted for on the assembly level by interpolating macroscopic cross sections as a function of depletion (MWD/MT) for each assembly. The fuel shuffling capability in the 2DB code allowed actual FNR operation to be simulated. The axial buckling term for the 2DB code used to approximate transverse leakage was based on a buckling and zonal buckling modifiers obtained from three-dimensional VENTURE calculations.

D. Control Rod Worth Calculations

FNR control (shim) rods are boron stainless steel containing 1.5 w/o natural boron. They are essentially black to thermal neutrons and cause a drastic thermal flux depression when inserted. The presence of such strong localized absorbers necessitates the use of transport theory codes to adequately describe the large flux gradients. However, in a small high leakage core like the FNR, control rod effects are not strictly local; therefore, whole core calculations are needed, but are prohibitively expensive for transport theory codes. To accurately treat both local and global

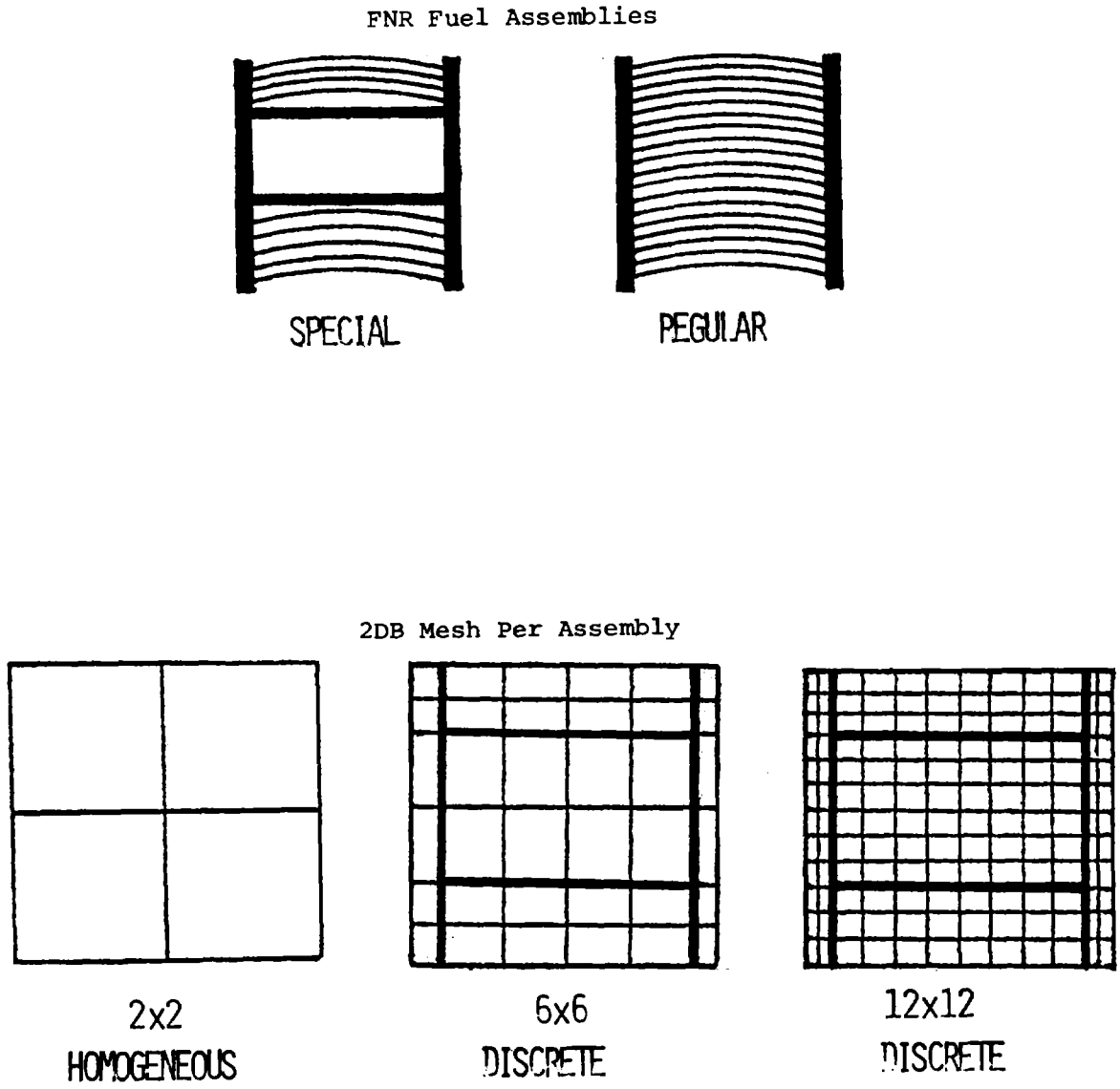

Figure 1 2DB Mesh Description

effects, transport theory codes were used for assembly level calculations to develop effective diffusion theory constants for global calculations.

Few-group constants for the control rod and surrounding water were obtained from the EPRI-HAMMER code for a cylindricized special assembly. Due to the strong spectral/spatial coupling in the rod it was necessary to obtain few-group cross sections for three control rod regions - a surface layer .1 cm thick, a second layer .3 cm thick, and the central region. Since few thermal neutrons reach the central region, the control rod perimeter, rather than volume, was preserved in the geometric representation. Few-group constants for the special element lattice and side regions were obtained from the EPRI-HAMMER calculations for one half of a special element in slab geometry.

To accurately model the local effects of an inserted rod, the two-dimensional transport code TWOTRAN was used in fine-mesh calculations for a special assembly surrounded on all sides by one half of a regular assembly. Three regions of the rod and the surrounding water were explicitly represented, while the surrounding lattice regions were homogenized.

To develop effective few-group diffusion theory constants for use in global 2DB calculations, the 2DB code was used for the same geometry as in TWOTRAN calculations, except that the control rod and surrounding water were homogenized. Both fast and thermal absorption cross sections were varied until the 2DB calculation yielded the same relative absorption in the control region as the TWOTRAN result in each group. The resulting few-group constants for the control region were then used in global 2DB calculations. Although the flux distribution within the control region differed from the

transport theory results, we believe the relative absorption in the control region and the flux in the surrounding fuel is accurately predicted in this scheme.

Control rod worth was then determined by comparing global 2DB calculations for the 6x6 mesh/assembly description with and without control rod inserted.

E. Calculation Methods for Temperature Coefficient of Reactivity and Xenon Reactivity Worth

Calculations of the temperature coefficient of reactivity and of reactivity worth of xenon poisoning were performed with global 2DB calculations with a 6x6 mesh/assembly description. The two-group cross sections for these 2DB cases were obtained from unit-cell calculations with the LEOPARD or the EPRI-HAMMER code, essentially following the basic scheme outlined in Section II.C. To facilitate the calculation of the various coefficients, several modifications have been made to 2DB and LEOPARD. A microscopic xenon calculation has been added to 2DB which allows the calculation of spatially dependent xenon concentrations and corresponding adjustment of the local macroscopic cross sections in the 2DB calculation.

The calculation of the isothermal coefficient of reactivity does not require any additional modifications because cross sections are simply generated at a different temperature input to LEOPARD. However, the power defect of reactivity represents the total of all reactivity effects induced by taking the reactor from a cold zero-power condition to normal operating conditions. Due to the spatially nonuniform temperature and density changes

involved, the power defect cannot be predicted solely on the basis of an isothermal temperature coefficient. Therefore, additional changes were necessary. In particular a restart capability has been added to LEOPARD to allow the recalculation of the spectrum at any depletion step with one or more variables changed from the base depletion calculation. LEOPARD then calculates the resultant deviation $\Delta\Sigma$ in all cross sections divided by the variable change $\Delta\xi$ and outputs the "derivative" cross section $(\frac{d\Sigma}{d\xi})$ as a function of depletion. The 2DB code then calculates the local change in the variable, e.g., the change in the moderator temperature from the nominal temperature, and multiplies the interpolated derivative cross section by this change and adds the increment to the base macroscopic cross section, which is itself interpolated as a function of depletion and fuel type. Extensive changes to 2DB were not needed because existing mixing routines in 2DB were utilized. The $\frac{d\Sigma}{d\xi}$ cross section is treated as a microscopic cross section, which is multiplied by the "density" $\Delta\xi$ and added to the base macroscopic cross section Σ_o: $\Sigma = \Sigma_o + (\frac{d\Sigma}{d\xi})\Delta\xi$.

III. VERIFICATION OF ANALYTICAL METHODS

A. Spectrum Calculations

The two cross section generation codes that have been utilized, LEOPARD and HAMMER, are well-verified codes and further effort to verify them was not warranted except for the application of LEOPARD to slab geometry. Since LEOPARD is a production code for pin cell geometry it was necessary to compare our modified version with a code capable of treating slab geometry. In particular we compared the slab version of LEOPARD with the HAMMER code for both LEU and HEU MTR-type fuel. Table 2 contains a comparison of the various

neutronics parameters and macroscopic cross sections for a unit cell calculation. In addition, the LEOPARD code has been verified against several critical assemblies, including the TRX rodded UO_2 and natural uranium slab lattices.[14] The agreement has been reasonable, and has further increased our confidence in the use of LEOPARD for routine calculations for MTR-type fuel configurations.

B. Global Calculations

To verify the accuracy of the analytic methods used in predicting core physics parameters for the HEU and LEU fuels the calculated results have been compared with experimental data from the Bulk Shielding Reactor (BSR)[15] and for various FNR core configurations. The comparisons for several FNR configurations summarized in Table 4 indicates the adequacy of the methods for calculating core criticality, power and thermal flux distributions, and control rod worth. Results of preliminary calculations simulating the power defect of reactivity data are also presented in this section.

The results presented in Table 4 indicate that core criticality is predicted accurately in our calculations. These calculations have revealed that considerable attention must be given to an accurate representation of the fuel geometry and of trace isotopes, such as U-236. Leakage in the axial direction in our two-dimensional (x-y) 2DB calculations was represented through the use of zone-dependent axial buckling obtained from three-dimensional VENTURE calculations. The resultant 2DB calculations are quite sensitive to the input buckling distribution and care must be taken when determining

Table 4 Experimental and Calculated Results for FNR Cores

Core Criticality

FNR Cycle	Mesh/Assembly	Measured	Calculated
146	6x6	1.000	1.003
183B	8x8	1.000	1.001

Assembly Power and Thermal Flux Distribution

FNR Cycle	Mesh/Assembly	Measurement	Locations Measured	RMS Deviation
67	6x6	Power	35	9.5%
152A	2x2	Thermal Flux	33	6.2%
157B	2x2	Thermal Flux	30	7.7%
159	2x2	Thermal Flux	34	7.1%
167A	2x2	Thermal Flux	33	4.5%
175D	2x2	Thermal Flux	22	7.2%
175D	8x8	Thermal Flux	22	7.4%
175D	12x12	Thermal Flux	22	8.0%
177B	2x2	Thermal Flux	22	5.5%

Total Control Rod Worth (% $\Delta k/k$)

FNR Cycle	Mesh/Assembly	Measured	Calculated	Deviation
17	6x6	6.57	6.41	-2.4%
67	6x6	6.24	6.30	+0.9%
91*	6x6	6.39	6.31	-1.1%
119	6x6	6.42	6.37	-0.7%
144	6x6	5.81	6.07	+4.5%
178	6x6	5.66	6.26	+10.4%

*New control rods installed

the transverse buckling for 2DB. The comparison of the calculated flux and power distributions with the FNR data given in Table 4 indicates reasonable agreement with RMS deviations in the range 4 - 10%. The comparison is based on the thermal flux data obtained with self-powered rhodium detectors at the core midplane and center of regular fuel elements. For Cycle 67, the power distribution was obtained from the measured temperature rise across each fuel assembly.

Control rod reactivity worth calculations were performed for six different FNR configurations. The method for obtaining the rod worths was discussed in Sec. II.D, except that the fuel depletion in the special fuel elements was also modeled. Accordingly, isotopic number densities for the lattice regions were taken from a LEOPARD depletion calculation for a special element at the corresponding burnup points. These number densities were then used in place of BOL number densities, and the sequence of HAMMER calculations described in Sec. II.D was repeated. Full-core 6x6 2DB calculations were then performed with all rods out and then separate runs were made with each of the three rods inserted. The calculated and measured rod worths are compared in Table 4.

The measured rod worths were determined from period measurements for rod positions in the upper half of the core. Considerable uncertainty exists in the measured worths due to the conversion from half rod to full rod worth and due to the use of an assumed effective delayed neutron fraction of .755%.[16] The calculated worths are in good agreement, although the increasing differences suggest that neglect of boron depletion over many years of operation may be a source of error. Despite these uncertainties, the basic approach for computing control rod worth appears valid for comparing rod worths in HEU and LEU cores.

A preliminary calculation of the FNR power defect has been performed using the methods described above. However, the 2DB calculation, being a two dimensional calculation, cannot explicitly account for the effect of axial variations in fuel and moderator temperatures. Therefore, as a first attempt we have neglected axial variations and have represented radial temperature profiles by assuming an average temperature for each fuel assembly, which was determined on the basis of a 2DB calculation (to determine relative power factors) and measured FNR core temperature drops and flow rates. With this model, the power defect was calculated to be $-.16\% \frac{\Delta k}{k}$, which may be compared with the experimental value of $-.21\% \frac{\Delta k}{k}$. We are currently attempting to improve our model, by including a typical axial power distribution into the analysis by weighting the calculated temperature changes in an appropriate fashion.

IV DESCRIPTION OF BATCH AND EQUILIBRIUM CORE MODELS

To provide meaningful and comprehensive comparisions of HEU and proposed LEU fuels, it is necessary to model both the intrinsic fuel properties and the FNR operating conditions. For this purpose, two core configurations were analyzed for both fuels. The first configuration is a batch core consisting of fresh fuel assemblies, while the second configuration is an equilibrium core. The batch core configuration allows a comparison of undepleted HEU and LEU fuels, while the equilibrium core allows comparison of depletion characteristics and shutdown margin for conditions typical of FNR operation. The batch core model illustrated in Figure 2 has 31 fresh fuel assemblies, with four special assemblies at control rod locations. The configuration is symmetric about the north/south midplane and was analyzed using half-core calculations.

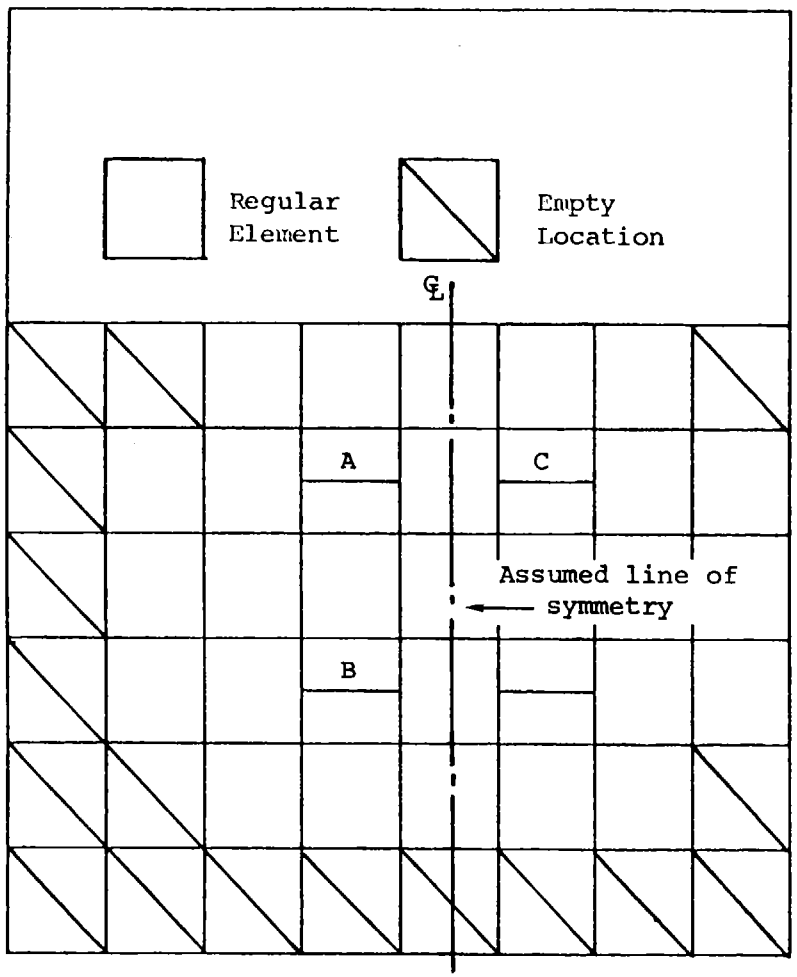

Figure 2 Batch Core Configuration

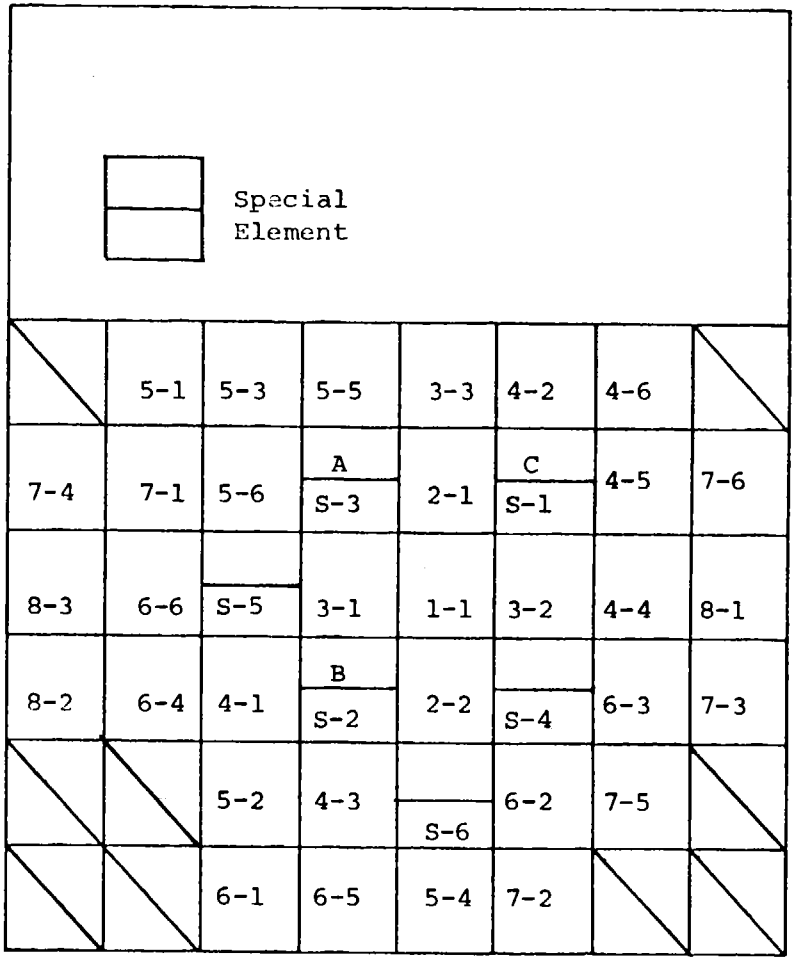

Figure 3 Equilibrium Core Loading Zones

Although the FNR core configuration and fuel shuffling pattern are, in practice, determined by operational requirements, an equilibrium core model was developed to allow a meaningful comparison of operating characteristics for the HEU and the proposed LEU cores. The equilibrium core shown in Figure 3 uses an in/out shuffling scheme with fresh elements loaded at the core center and moved outward to the core edge. This scheme maximizes the reactivity worth at the core center, thus maximizing the control rod worth to achieve the required 3% $\Delta k/k$ shutdown margin. To compare different fuel types in the equilibrium core, the end of cycle (EOC) k_{eff} was preserved between different cases. Preserving EOC k_{eff} provides the most realistic comparison of different fuel types, because it attempts to model actual FNR operation where a core is depleted until the shim rods are nearly fully withdrawn. Along with preserving the EOC k_{eff} the core size is also maintained constant. These two criteria essentially determine the maximum fuel burnup for a given fuel design. To achieve any higher burnup would require that the core size be increased in order to maintain criticality. Once the maximum fuel burnup is determined by preserving k_{eff} with a fixed core size, calculations must be performed to verify that the core configuration has the required 3.0% $\Delta k/k$ shutdown margin. Although the fuel burnup and power distribution are roughly constant during each equilibrium cycle, our equilibrium core configuration is chosen in such a way that the core configuration repeats every sixth cycle.

The shuffling pattern in the equilibrium cycles divides the 33 regular fuel element locations into eight loading zones as shown in Figure 3 . Each regular element loading zone corresponds to core locations having

nearly equal fuel burnup, although not necessarily equal burnup rates. New fuel is loaded into Zone 1 and depleted fuel is discharged from Zone 8. At the start of each cycle, one new element is loaded into Zone 1, and the element in Zone 1 is moved to Zone 2. The fuel shuffling continues to Zone 8, where elements are discharged. The eight-zone shuffling pattern for the regular elements is shown in Figure 4.

The shuffling pattern for the special fuel elements is different because there are six special element locations. A new special element is added and a depleted element is discharged only every sixth cycle. With this shuffling pattern a new special element is placed in Special-Zone 1 at the start of cycle 1. The element removed from Special-Zone 1 is placed in ex-core storage for one cycle and then placed in Special-Zone 2 at the start of cycle 2. The sequence continues until the start of cycle 6 when the element from storage is placed into Special-Zone 6 and a depleted special element is discharged from the core. This shuffling pattern for special elements is shown also in Figure 4.

V. CHARACTERISTICS OF THE EQUILIBRIUM CORE MODEL AND FNR OPERATION

The equilibrium core model was designed to be typical of the actual FNR operation. Many characteristics of the FNR operation are well represented in the equilibrium core analysis. In fact, a modified version of the equilibrium core shuffling scheme has been implemented at the FNR and has proven to be a practical and efficient scheme for loading fuel elements. Nonetheless there are differences between the equilibrium core model and actual FNR operation. These differences exist mainly because FNR operation is more flexible than the equilibrium model. Fuel

Figure 4. Equilibrium Core Shuffling Scheme

Regular Fuel Elements

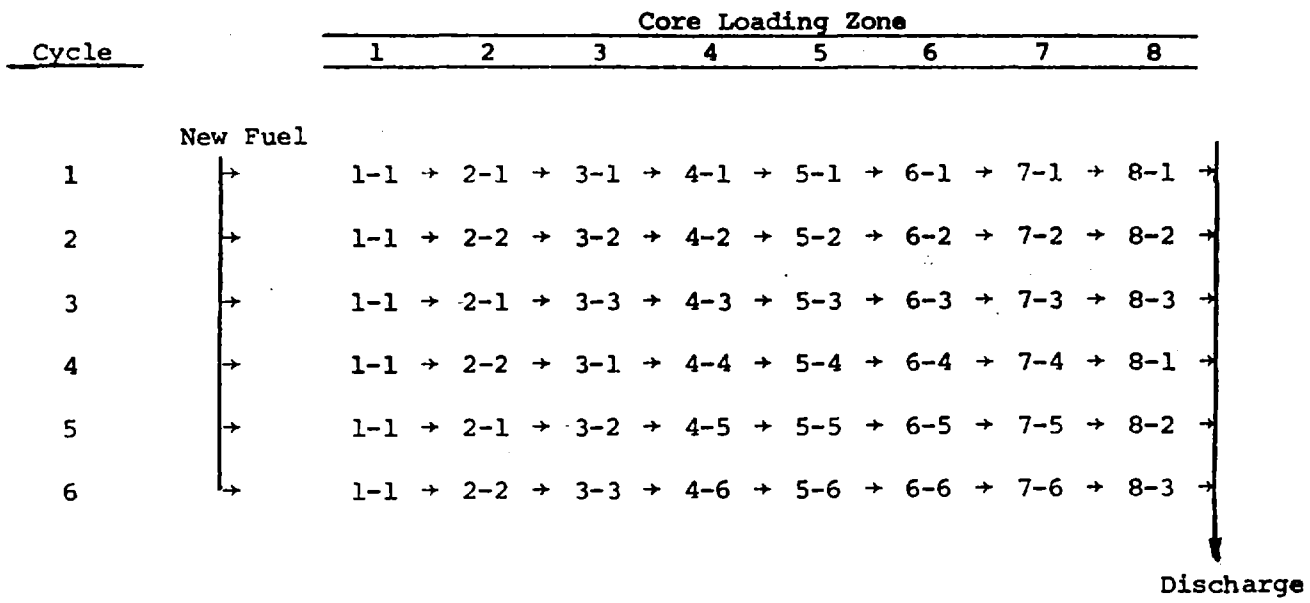

Special Fuel Elements

Cycle	Storage		Core Loading Zone		Storage
1	New fuel	→	S-1	→	X_1
2	X_1	→	S-2	→	X_2
3	X_2	→	S-3	→	X_3
4	X_3	→	S-4	→	X_4
5	X_4	→	S-5	→	X_5
6	X_5	→	S-6	→	Discharge

elements need not be shuffled in any fixed pattern and the core configuration does not repeat periodically. This section describes characteristics of the equilibrium model and actual FNR core configurations, and also explains important differences between the equilibrium analysis and actual operation.

To verify the practicability of the equilibrium model, Table 5 presents a comparison of the calculated equilibrium core parameters and actual core parameters based on FNR operation. The comparisons indicate that the proposed equilibrium cycle represents a reasonably practical configuration for comparing the HEU and LEU fuel designs. On the average fuel elements are shuffled just as often in both cores. The calculated control rod worths for the equilibrium core compare well with the rod worths measured in the FNR.

The cycle length comparisons for the equilibrium and operating cores in Table 5 point out a difference between analytic models and actual operations. In the equilibrium core model, cycle length is determined by the discharge fuel burnup averaged over the regular and special fuel elements. In contrast, the FNR operating cycle length is the time interval between shim rod calibrations, which are required by technical specifications whenever more than three fuel elements are shuffled. In calculations comparing the HEU and LEU fuels the parameter most indicative of the time between control rod calibrations or operating cycle length is the burnup reactivity change rate, rather than the equilibrium core cycle length. With a constraint on the allowable core excess reactivity, the length of time the core can be maintained critical without shuffling more than three fuel elements, thereby requiring rod recalibration, is determined

Table 5 Comparison of Equilibrium Core and Actual FNR Parameters.

	Operating Experience*	HEU Equilibrium
Operating cycle length (days)	17.6	—
Equilibrium cycle length (days)	—	11.0
Average number of element shuffles/day	.82	.80
Average discharge burnup (MWD/element)		
Regular	19.4	19.2
Special	19.5	16.9
Calculated k_{eff}		
Range	1.022-1.026	1.020-1.032
Average	1.024	1.025
Shim rod worth (%Δk/k)		
Rod A	2.20	2.08
Rod B	2.21	2.24
Rod C	2.00	2.17
Total	6.41	6.49

*Averaged from Oct. 78 to Nov. 79

by the fuel burnup reactivity change rate.

VI. CORE NEUTRONIC ANALYSES FOR THE HEU AND LEU FUELED CORES

The important neutronics parameters analyzed for the HEU and LEU fueled cores are the temperature coefficients of reactivity, xenon reactivity, control rod worth, discharge burnup, and the shutdown margin. Comparisons of these neutronic parameters for the batch core and equilibrium core configurations should provide a basis for assessing the impact of LEU fuel on FNR performance and utilization. Before discussing the results of these comparisons, the actual HEU and LEU fuel configurations will be discussed.

A. LEU and HEU Fuel Description

The selection of the LEU fuel design was based on extensive generic studies and survey calculations carried out by Argonne National Laboratory[17-19], The University of Michigan, and others. In addition, constraints were imposed on the final design as a result of the specific FNR system configuration, FNR operational considerations, and the need to obtain approval from the NRC of an amendment to the current FNR operating license. These constraints, which are unique to the FNR, had to be factored into the final LEU design.

Based on the above considerations, the LEU fuel design selected for the FNR was identical in all external dimensions to the HEU fuel as shown in Table 6 . The conversion to LEU fuel results in an increase in U-238 loading by a factor of nearly 5 and an increased U-235 loading to overcome the increased capture in U-238. To accommodate the additional uranium loading, the fuel meat thickness was increased 50% with a corresponding reduction in the

Table 6 HEU and LEU Fuel Designs

	HEU	LEU
Fissile enrichment	93%	19.5%
Regular element fissile loading (gm)	140.0	167.3
Uranium density in fuel meat (w/o)	14.1%	42%
Fuel plates per element	18	18
Fuel meat thickness (in)	.020	.030
Clad thickness (in)	.020	.015
Fuel plate thickness (in)	.060	.060
Water Channel thickness (in)	.117	.117

cladding thickness, hence keeping a constant fuel plate thickness. The FNR licensing considerations dictated the use of fuel with at most 42.0 w/o uranium loading, which is considered to be an acceptable fuel design based on experience and testing to date. Using 19.5% enriched uranium, the above LEU design has 167.3 g of U-235 per fuel element, and results in the same excess reactivity for the batch core as the HEU fuel design, as desired.

B. Flux and Power Distributions

Calculated power distributions for both HEU and LEU cores are compared in Figures 5 and 6 for batch cores and equilibrium cores, respectively. Examination of these figures reveals only minor changes between LEU and HEU cores. The largest change in assembly power, a 3% relative increase, occurs ior special element locations. Additionally, there is a small shift in the power distribution away from the heavy water tank and toward a slightly improved overall symmetry about the center. There is no evidence of changes which would required detailed thermal-hydraulic analysis; in fact, the ratio of peak to average assembly power is slightly reduced.

The calculated fast and thermal flux distributions are compared in Figures 7 and 8 for the batch and equilibrium cores, respectively. The figures indicate that the fast flux distribution is perturbed very little with LEU fuel. This is to be expected because the fast neutron production and removal rates are nearly equal for the two cores. The fast neutron production is approximately constant because the core power

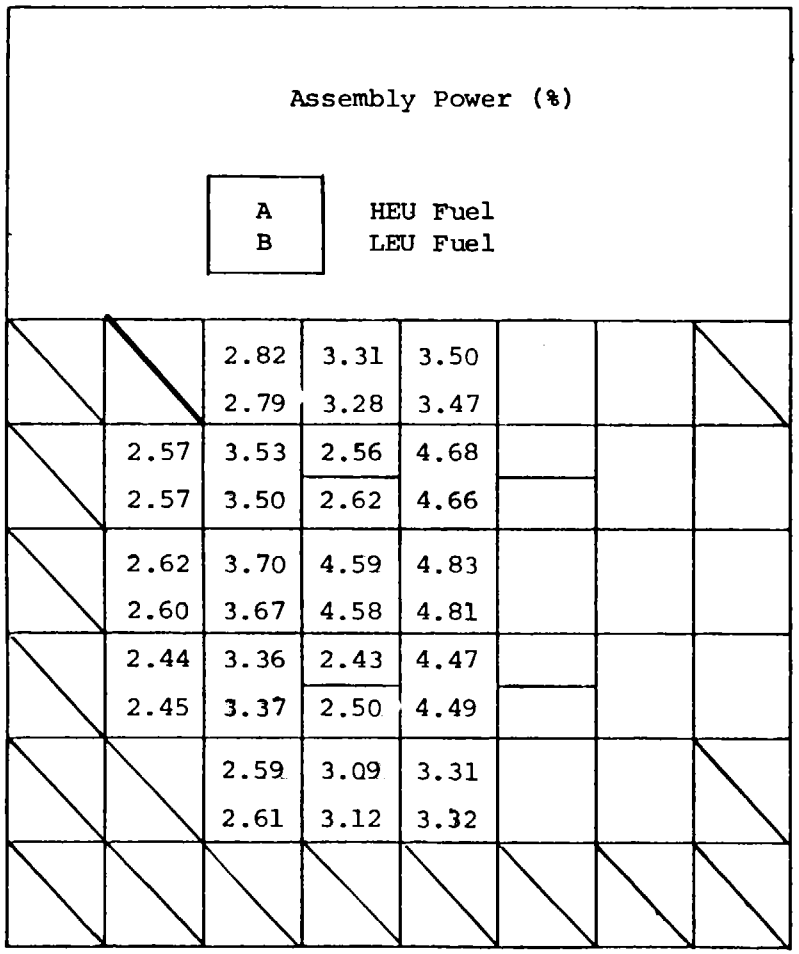

Figure 5 Assembly Power Distribution for HEU and LEU Batch Cores

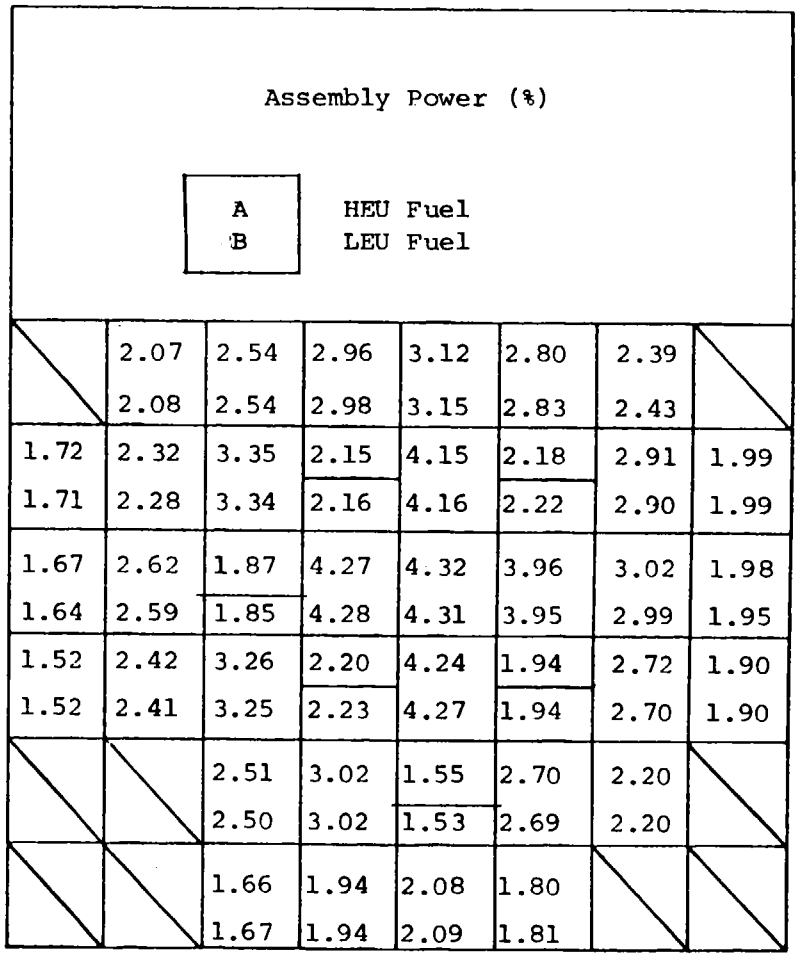

Figure 6 Assembly Power Distribution for HEU and LEU Equilibrium Cores

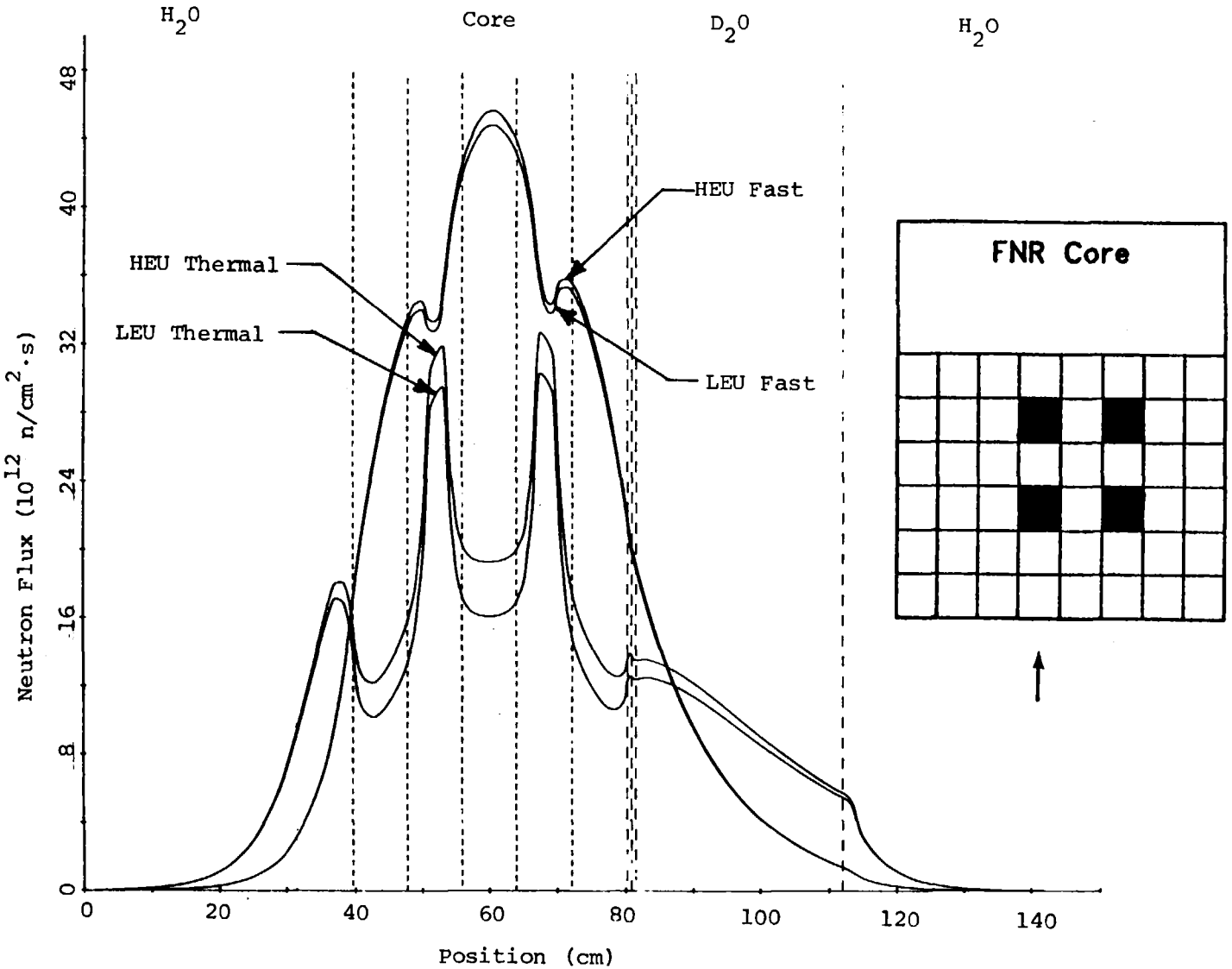

Figure 7 Neutron Flux Distribution for Batch Cores

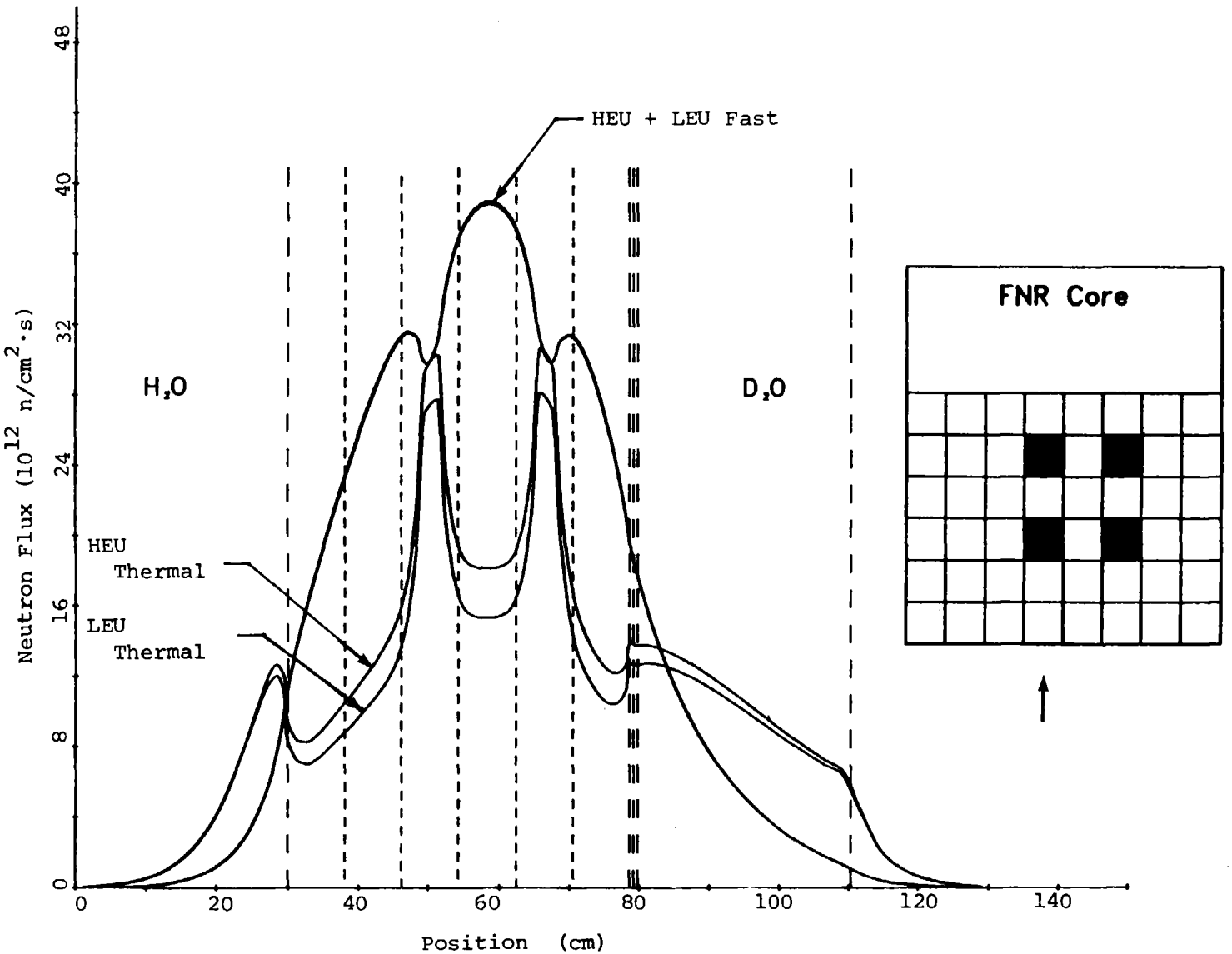

Figure 8 Neutron Flux Distribution for Equilibrium Cores

is held constant at 2 MW, while the fast neutron removal rate is nearly constant due to the similar moderating properties of the two cores. That is, the water channel dimensions are the same.

However, one expects to see significant changes in the incore thermal flux distributions between the HEU and LEU fuels. For a well-moderated thermal reactor at constant power, the thermal flux is nearly inversely proportional to the fissile loading, hence one expects a reduction in thermal flux for the LEU core. This effect is readily apparent in Figures 9 and 10 where the thermal flux in regular fuel elements is seen to decrease by about 18%. For special fuel elements, the reduction in thermal flux is only about 12%. This mitigation in the thermal flux decrease results from the effect of the thermal flux peaking in the large waterhole. This peak is primarily dependent on the fast flux, which is not significantly different between the LEU and HEU fuels. Since the thermal flux level within the special element will be affected by the waterhole peaking, the overall effect is to mitigate the decrease in thermal flux. As noted for the power distribution, there is a slight shift in thermal flux away from the heavy water tank toward a slightly improved overall symmetry about the center.

Excore thermal flux levels are important in the FNR because samples are generally irradiated in the reflector regions. In particular the heavy water reflector is of greatest interest because thermal neutron beam tubes extend from the tank to the laboratory areas. Comparisons of the thermal flux levels in the light water reflector show a flux depression varying from zero to 6%. At distances well into the light water reflector, there is no change because the primary source for

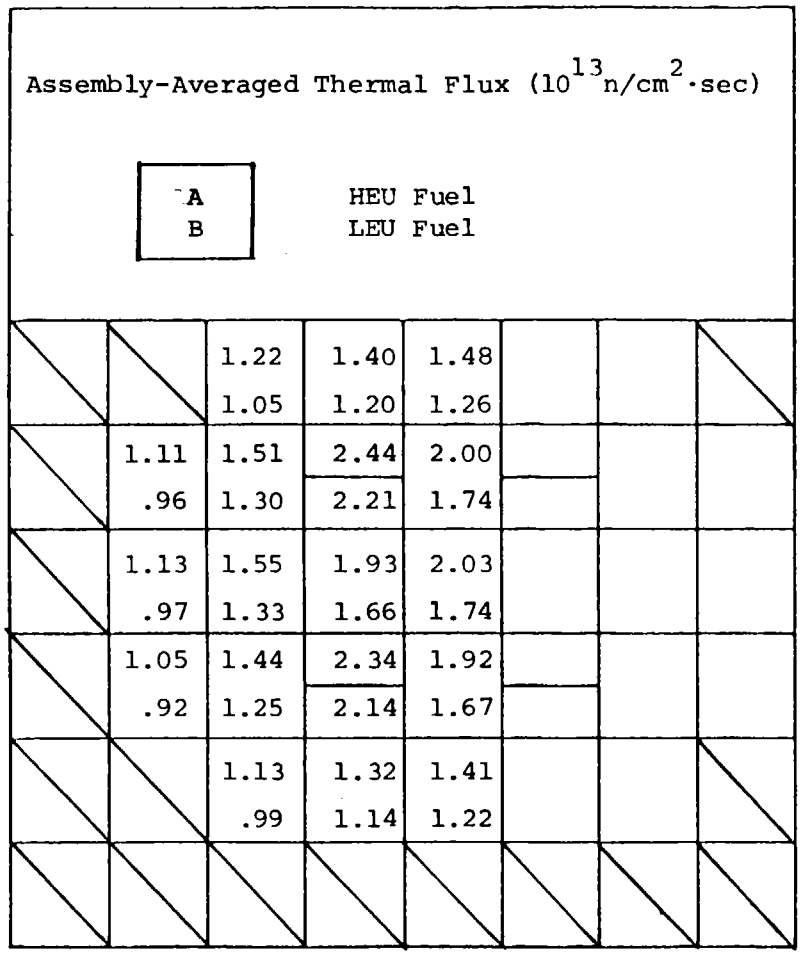

Figure 9 Thermal Flux Distribution for HEU and LEU Batch Cores

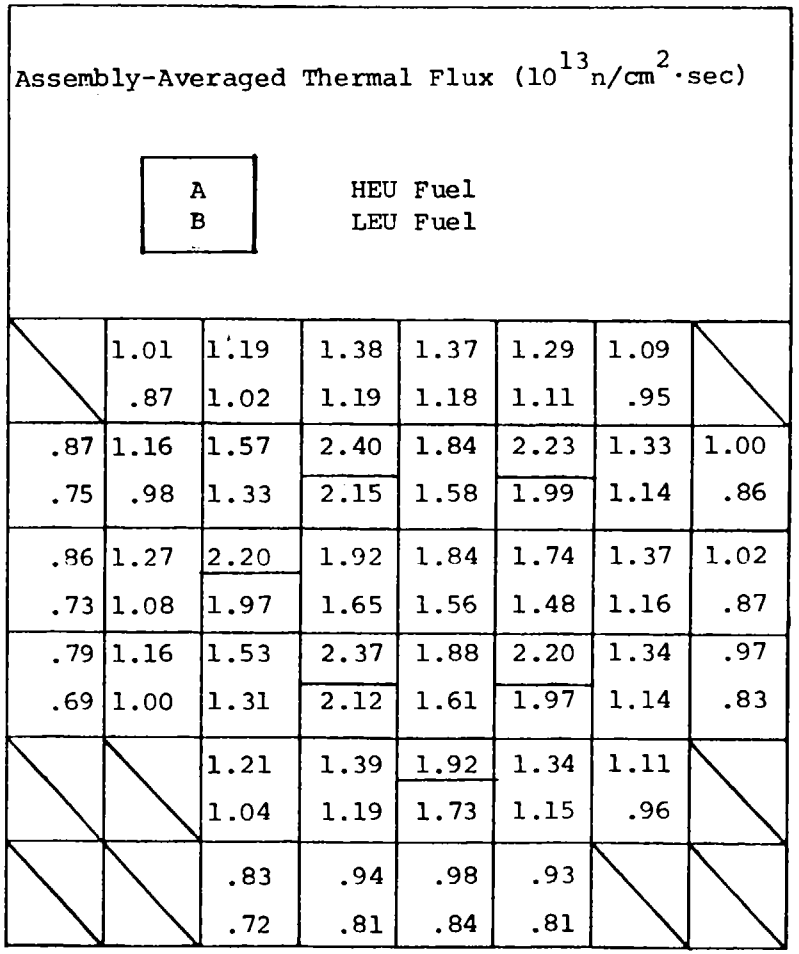

Figure 10 Thermal Flux Distribution for HEU and LEU Equilibrium Cores

thermal neutrons is the slowing down of fast neutrons leaking from the core. At locations closer to the core the contribution to the thermal flux due to thermal leakage from the core is larger and, since the thermal leakage is decreased by the increased fuel loading, there is a correspondingly greater decrease in the thermal flux. Consistent with this explanation, the relative thermal flux in the heavy water tank is depressed somewhat more (4-8%) than in the light water reactor due to the increase in the relative contribution of thermal leakage to the heavy water tank thermal flux.

C. Temperature Coefficient of Reactivity and Power Defect

The isothermal temperature coefficient of reactivity was computed for the batch core model to be -8.4 pcm/°F for the HEU fuel and -12.6 pcm/°F for the LEU fuel. The large increase is due almost exclusively to the fuel Doppler effects. For the HEU fuel, fuel Doppler effects are negligible due to the small amount of U-238 present. For the LEU fuel, the large amount of U-238 increases resonance absorptions in U-238, resulting in much larger sensitivity to fuel temperature. The principal contribution to the temperature coefficient of reactivity for both the HEU and LEU configurations is, however, the effect of the reduction in moderator density on leakage and moderation.

As discussed earlier, the procedure for calculating the power defect has not been fully developed, and a comparison of the difference in the power defect for the HEU and LEU cores has not been made. However, a preliminary estimate has been made based on the observation that the increase in the fuel Doppler effect is the principal difference in the temperature effects between the HEU and the LEU designs. The change in

power defect of reactivity is estimated in the present analysis on the basis of calculated temperature coefficients. Based on an average core temperature rise of 7°F, the power defect for the LEU fuel is estimated to be about .03% Δk/k larger in magnitude than for HEU fuel. For a typical FNR configuration, the excess reactivity required to overcome thepower defect would thus change from a measured value of .21% Δk/k for HEU to .24% Δk/k for LEU.

D. Xenon Reactivity Worth

The xenon reactivity worths of the HEU and LEU fuels are compared in Tables 7 and 8 for the batch and equilibrium core models, respectively. For these cores the xenon worth is 4-6% lower for the LEU than the HEU fuel. There are two competing effects responsible for this decrease: First, the larger U-235 loading for the LEU core results in lower incore thermal flux levels, with a greater (10-12%) xenon concentration. Second, the increased fuel loading gives the LEU core a larger neutron absorption cross section. As total core absorption is increased, the fractional absorption in xenon, and thus the xenon reactivity worth, is decreased. Although these two effects tend to cancel one another, the latter effect dominates and xenon reactivity worth is lowered by about .1% Δk/k.

E. Fuel Cycle Analyses

Equilibrium fuel cycle analyses have been performed for the HEU and LEU cores and the results are presented in Table 9. The comparison of discharge fuel burnup,which indicates a 50% increase for LEU fuel, should be viewed with some care because of the extreme sensitivity of

Table 7 Batch Core Reactivity Comparisons

	HEU	LEU	Change
Cycle length (days)	10.0	10.0	
Burnup reactivity change rate (%Δk/k/day)	-.028	-.02	-28%
Shim rod worth (%Δk/k)			
A Rod	2.37	2.26	
B Rod	2.23	2.12	
C Rod	2.37	2.26	
Total	6.97	6.64	-4.7%
Excess reactivity required (%Δk/k)			
Xenon poisoning	2.50	2.40	-4.0%
Burnup effect	0.28	0.21	
Power defect	0.21	0.24	
Total	2.99	2.85	-4.7%
Shutdown margin (%Δk/k)	3.98	3.79	-4.0%

Table 8 Equilibrium Core Reactivity Comparisons

	HEU	LEU	Change
Cycle length (days)	11.0	16.5	50%
Burnup reactivity change rate (%Δk/k/day)	-.028	-.021	-24%
Shim rod worth (%Δk/k)			
A Rod	2.20	2.14	
B Rod	2.21	2.15	
C Rod	2.00	1.96	
Total	6.41	6.25	-2.5%
Excess reactivity required (%Δk/k)			
Xenon poisoning	2.26	2.17	-4.0%
Burnup effect	.31	.37	
Power defect	.21	.24	
Total	2.78	2.78	0%
Shutdown margin (%Δk/k)	3.63	3.47	-4.4%

Table 9 Equilibrium Core Fuel Cycle

	HEU	LEU	Change
Cycle length (days)	11.0	16.5	50%
Discharge burnup (MWD/element)			
Regular	19.2	28.7	49%
Special	16.9	25.9	53%
Regular element Fissile loading (gm)			
Fresh	140.6	167.3	20%
Discharge	116.6	134.3	15%
Core loading Beginning of cycle (gm)			
Fissile	4550	5320	17%
U-235	4549	5260	16%
Burnup reactivity change rate (% $\Delta k/k$/day)	.0279	.0211	-24%

discharge fuel burnup to core reactivity for the FNR core. For example, in an equilibrium core analysis comparing two LEU core configurations, a 0.5% $\Delta k/k$ change in eigenvalue resulted in a 15% increase in the discharge burnup. This sensitivity is a consequence of the relatively low fissile depletion obtained in the FNR core. Typically only 17% of the initial fissile inventory is depleted from the HEU fuel elements before discharge. A significant change in the discharge fissile depletion can be achieved with only a small relative change in the total core fissile inventory, which is, of course, proportional to core criticality. Thus, the predicted discharge burnup is very sensitive to the calculated core criticality. In addition, this sensitivity is magnified by the in/out shuffling pattern used at the FNR. This shuffling scheme loads the depleted fuel elements into regions of lower neutron importance. Thus, changes in the discharge burnup have a relatively smaller effect on core criticality than with other shuffling schemes. Because core size and core criticality are directly related, discharge fuel burnup is also sensitive to core size. Therefore, to provide valid comparisons a fixed core size was used in our equilibrium core analysis. Calculations for both the batch and equilibrium cores indicate a decrease in the burnup reactivity change rate with LEU fuel. The decrease in reactivity change rate is a consequence of two factors. Most importantly, the core fissile loading is higher with LEU fuel, so that the fractional fuel depletion rate, and the burnup reactivity change rate, are lowered. Production of Pu-239 in the LEU fuel also causes a decrease in the burnup reactivity change rate. Fuel depletion calculations indicate that the Pu-239 production rate is approximately 8% of the U-235 loss rate in the LEU core. This may translate into a 10-15% decrease in the burnup reactivity change rate, depending on the

reactivity worth of Pu-239 vs. U-235. Comparisons of reactivity changes in the HEU and LEU batch cores show that during the first 50 full power days of operation reactivity is lost more rapidly than at later times due to the effects of xenon and samarium, as well as fuel depletion. Once this initial transient has passed the burnup reactivity change rates are nearly constant and approximately 25 to 30% lower in the LEU core. In the equilibrium core calculations the burnup reactivity change rate is affected by the fuel burnup distribution as well as total core fissile inventory. For this equilibrium core model the burnup reactivity change rate is decreased by 24% with the LEU fuel. Thus, as explained earlier a 30% increase in the FNR operating cycle length is expected.

F. Control Rod Worth

Shim rod reactivity worth comparisons for the A, B, and C rods are given in Tables 7 and 8. The LEU batch core comparison shows a 5% relative decrease in shim rod worth. This decrease in rod worth may be explained qualitatively by noting that, to a good approximation, the FNR rods are black and, for a black rod control, rod worth is nearly proportional to the product of the control surface area and the thermal diffusion length in the surrounding fueled region.[20] Since the thermal diffusion length in the LEU core is 2.05 cm vs. 2.18 cm in the HEU core, this simple model predicts a decrease in rod worth of approximately 6%, which may be compared with the calculated 5% decrease in rod worth for the batch core configuration. In the equilibrium configuration the total rod worth decreases by only 3%. This smaller decrease in rod worth indicates that factors other than the shorter thermal diffusion length are also affecting the calculated rod worth. Rod worth calcu-

lations for various equilibrium cores show that rod worth is also affected by the discharge fuel burnup. As discharge burnup in the outer fuel elements is increased, the core fissile loading and core reactivity worth distribution shift toward the core center causing the rod worth to increase. Thus the higher discharge burnup in the LEU equilibrium core has a mitigating effect on the decrease in rod worth, and the net effect is a 3% decrease in total worth.

G. Comparison of Shutdown Margin

The most significant safety parameter related to core physics analysis is the shutdown margin. This parameter is obtained by subtracting the positive core excess reactivity required to overcome xenon poisoning, fuel depletion, and the power defect from the total control rod reactivity worth. The present technical specifications require that the shutdown margin be at least 3.0% $\Delta k/k$. Any difference between the estimated shutdown margin and the limiting value represents excess reactivity available for experiments.

For the LEU batch core, it is seen from Table 7 that the lower excess reactivity requirement is overshadowed by the decrease in control rod reactivity worth. The shutdown margin of 3.79% Δ k/k is lower than for the HEU core, but is still well above the 3% $\Delta k/k$ requirement. Additionally, with the most reactive rod fully withdrawn, the shutdown margin is 1.53% $\Delta k/k$, well in excess of the .75% $\Delta k/k$ required.

Comparing the HEU and LEU equilibrium core results in Table 8 shows that the shutdown margin decreases slightly for the LEU core. The computed value of 3.47% $\Delta k/k$ is well in excess of the 3.0% $\Delta k/k$ requirement. Also, the shutdown margin with the most reactive control rod fully withdrawn is 1.32% $\Delta k/k$, well above the .75% $\Delta k/k$ required.

VII. ALTERNATIVE LEU FUEL DESIGNS

The LEU fuel design was selected for the full core demonstration based on a criterion of creating minimum perturbations in reactor performance. To determine effective ways of improving core performance, e.g., the core fuel burnup, control rod worth, and excore flux levels, several alternative LEU fuel designs have also been studied.

This section presents results of an equilibrium core study comparing the LEU fuel with an alternative higher loaded fuel design. The two fuel designs are compared in Table 10 . The fissile loading for the alternative fuel design has been increased to 175 gm by increasing the uranium density in the fuel meat, without changing element dimensions. The important conclusion of this alternative fuel design study is that it may be possible to significantly increase fuel burnup without degrading other reactor performance characteristics.

The equilibrium core power and thermal flux distributions for the two fuels are compared in Figures 11, 12 and 13. The power distribution comparisons show only a slight shift for the higher loaded fuel, despite the increase in fuel burnup at the core edges. A maximum increase of about 2% in assembly power occurs near the core center and the heavy water tank. The thermal flux distribution comparison shows a maximum decrease of less than 3%, suggesting that the flux depression caused by the higher loading is partially mitigated by the higher fissile depletion.

Equilibrium core calculations predict a 26% increase in cycle length and discharge burnup for the 175 gm fuel. As explained earlier, the higher discharge burnup results because the fuel can be depleted longer while maintaining a critical equilibrium configuration. The 175 gm fuel

Table 10 LEU Fuel Design Comparisons

	Reference Design	Alternative Design	Change
Enrichment	19.5%	19.5%	0%
Regular element fissile loading(gm)	167.3	175.0	4.6%
Uranium density in fuel meat	42.0%	43.9%	4.6%
Element dimensions	——	——	0%
Equilibrium cycle length (days)	16.5	20.8	26%
Discharge burnup (MWD/element)			
Regular	28.7	36.4	27%
Special	25.9	32.5	24%
Burnup reactivity change rate (%Δk/k/day)	.0211	.0207	-2%
Shim rod worth (%Δk/k)			
A Rod	2.14	2.15	
B Rod	2.15	2.14	
C Rod	1.96	2.00	
Total	6.25	6.29	0.6%
Excess reactivity required (%Δk/k)			
Xenon poisoning	2.17	2.15	
Burnup effect	.37	.43	
Power defect	.24	.24	
Total	2.78	2.82	1.4%
Shutdown margin (%Δk/k)	3.47	3.47	0%

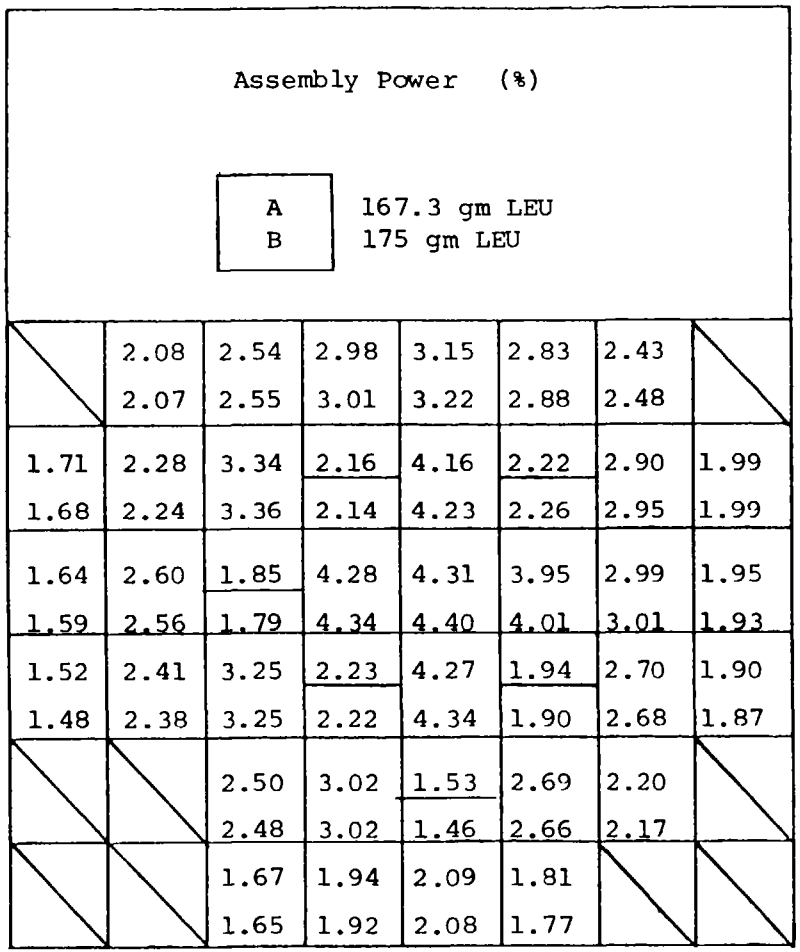

Figure 11 Power Distribution for 167.3 and 175 gm LEU Equilibrium Cores

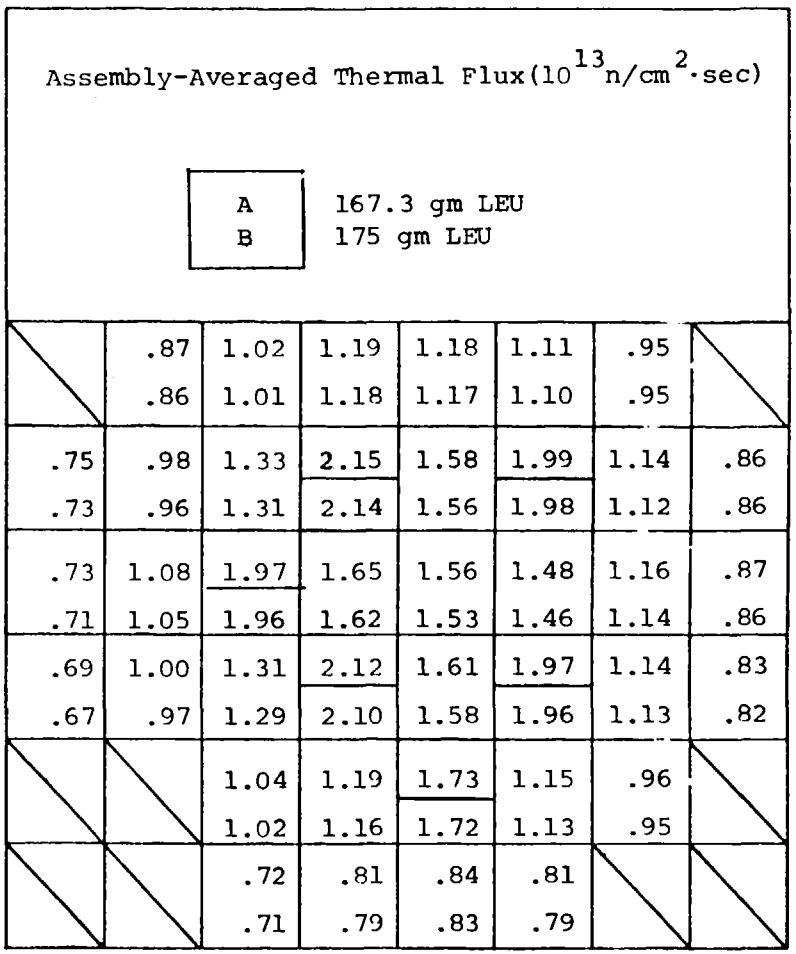

Figure 12 Thermal Flux for 167.3 and 175 gm LEU Equilibrium Cores

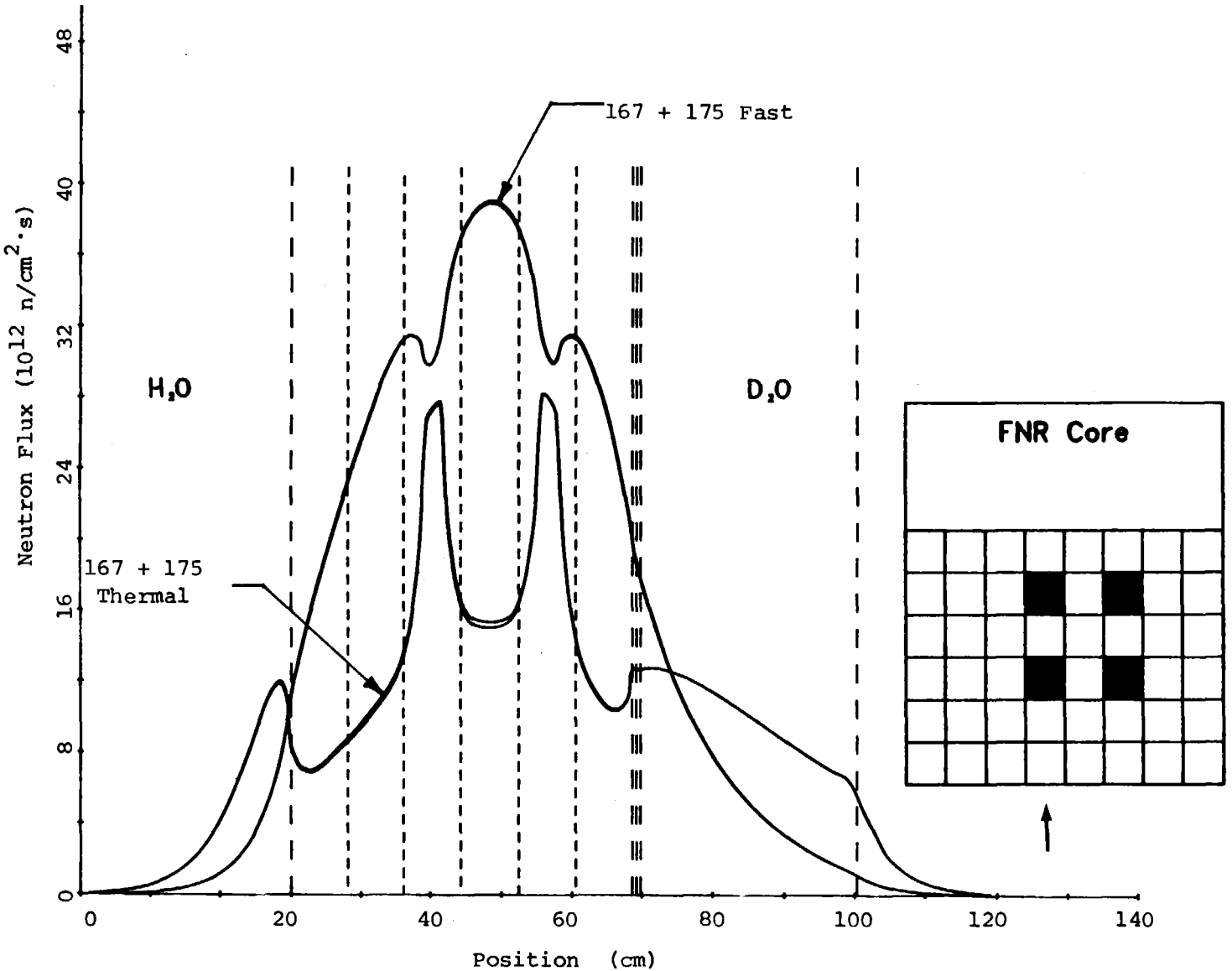

Figure 13 Neutron Flux Distribution for 167.3 and 175 gm LEU Fuels

is initially more reactive because of the higher fissile loading, and loses reactivity due to fuel burnup at a slower rate, as seen by the 2% decrease in burnup reactivity change rate. As noted earlier, however, care must be taken in interpreting these results because of the extreme sensitivity of discharge fuel burnup to core reactivity for the FNR.

Calculations of the reactivity effects for the two LEU fuels predict no change in shutdown margin with the higher loaded fuel. The control rod worth increases by an almost insignificant amount because the higher core edge depletion tends to increase core center reactivity worth. Thus the shutdown margin, as well as the core power and thermal flux distribution, are not significantly degraded even though the discharge burnup is considerably higher for the 175 gm fuel design.

VIII. SUMMARY

A 19.5% enriched fuel design was selected and is being fabricated as part of the FNR demonstration project. The fuel has a 167.3 gram fissile loading and 18 fuel plates per assembly. To accommodate the increased uranium content without changing fuel plate or assembly dimensions, the uranium loading in the fuel meat has been increased to 42 w/o and the fuel thickness has been increased 50% while decreasing the clad thickness.

Extensive efforts have been devoted to developing calculational methods for analyzing HEU and LEU fueled research reactors. These methods make use of existing well verified computer codes whenever possible and have been verified by comparison with data from several research reactor configurations.

To study all expected effects, the HEU fuel and LEU fuel were analyzed and compared in both batch and equilibrium core models. These comparisons serve to quantify predictions made on physical grounds : The higher fissile loading required to overcome the additional U-238 absorptions results in a large decrease in the in-core thermal flux. Thermal flux levels in the reflector are depressed to a lesser degree because the fast neutron leakage is nearly constant. The power distribution is not perturbed to a significant degree. The equilibrium cycle length and discharge fuel burnup are predicted to increase because the LEU core can be depleted longer while maintaining core criticality. There is a small decrease in the xenon worth and control rod worth caused by higher core absorption. Comparisons for the equilibrium cores indicate that the reduction in rod worth may be mitigated by the increased fuel burnup of the LEU core. Most importantly the comparisons predict no significant change in the core shutdown margin.

The analytic methods described in the paper have provided a reasonable assessment of the impacts of LEU fuel on FNR performance. However, there remain areas which deserve further study and additional refinement. Some specific items currently being investigated at The University of Michigan are:

1) Development of a new data library for the LEOPARD code based upon ENDF/B-IV data.
2) Investigation of optimal equilibrium core configurations using linear/dynamic programming concepts.
3) Continued investigation of discrepancies between measured and predicted rod worths, with a careful examination of possible boron depletion effects.
4) Calculation of β_{eff}, the effective delayed neutron fraction, for both HEU and LEU cores.

5) Refinement of the power defect calculation to include non-uniform axial effects.

6) Refinements in the determination and use of burnup dependent non-lattice peaking factors for the LEOPARD code.

7) Extensive analysis of the leakage flux levels in the FNR heavy water tank and beam port locations. Calculations are planned using both discrete ordinates and Monte Carlo methods.

REFERENCES

1. D. Wehe and J. S. King, "The FNR HEU-LEU Demonstration Experiment", (to be presented at this conference).

2. H. Komoriya, J. C. Lee, and W. R. Martin, Trans. Am. Nucl. Soc., 32, Suppl. 1, 31 (1979).

3. F. B. Brown, D. C. Losey, D. K. Wehe, J. C. Lee and W. R. Martin, Trans. Am. Nucl. Soc., 33, 746 (1979).

4. D. C. Losey, F. B. Brown, W. R. Martin, J. C. Lee, and H. Komoriya, Trans. Am. Nucl. Soc., 33, 748 (1979).

5. W. Kerr, et al., "Low Enrichment Fuel Evaluation and Analysis Program, Summary Report for the Period January 1979-December 1979", University of Michigan Report (Jan. 1980).

6. D. C. Losey, F. B. Brown, J. C. Lee and W. R. Martin, Trans. Am. Nucl. Soc., 34, 569 (1980).

7. R. F. Barry, "LEOPARD - A Spectrum Dependent Non-Spatial Depletion Code", WCAP-3269-26, Westinghouse Electric Corporation (Sept. 1963).

8. J. Barhen, W. Rothenstein, E. Taviv, "The HAMMER Code System", NP-565, Electric Power Research Institute (October 1978).

9. W. W. Little, Jr. and R. W. Hardie, "2DB User's Manual-Revision I", BNWL-831 REV1, Battelle Pacific Northwest Laboratory (February 1969).

10. W. W. Engle, Jr., "A User's Manual for ANISN, a One-Dimensional Discrete Ordinates Transport Code with Anisotropic Scattering", K-1693, Oak Ridge Gaseous Diffusion Plant (March 1967).

11. K. D. Lathrop and F. W. Brinkley, "TWOTRAN-II - An Interfaced Exportable Version of the TWOTRAN Code for Two-Dimensional Transport", Los Alamos Scientific Laboratory, LA-4848-MS (1973).

12. D. R. Vondy, T. B. Fowler, and G. W. Cunningham, "VENTURE: A Code Block for Solving Multigroup Neutronics Problems Applying the Finite-Difference Diffusion Theory Approximation to Neutron Transport", ORNL-5062 (1975).

13. M. H. Theys, Nucl. Sci. Eng., 7, 58 (1960).

14. J. Hardy, D. Klein, and J. J. Volpe, "A Study of Physics Parameters in Several Water-Moderated Lattices of Slightly Enriched and Natural Uranium:, WAPD-TM-931, Westinghouse Electric Corporation (March 1970).

15. E. B. Johnson, "Power Calibration for BSR Loading 33", CF-57-11-30, Oak Ridge National Laboratory (1957).

16. J. L. Shapiro, "The Void Coefficient in an Enriched, Water Reactor", Nucl. Sci. Eng., 12, 449 (1962).

17. H. Komoriya to J. L. Snelgrove, "Reduced Enrichment Fuel Element Loading Calculations for the Ford Nuclear Reactor", Argonne National Laboratory Internal Memorandum (February 14, 1979).

18. J. E. Matos and K. E. Freese, Trans. Am. Nucl. Soc., 33, 739 (1979).

19. H. Komoriya, Trans. Am. Nucl. Soc., 33, 745 (1979).

20. J. J. Duderstadt and W. R. Martin, Transport Theory, Wiley-Interscience, New York (1979).